

Effect of 2-D regular channels and their configurations on properties of ceramic preforms

Osayande L. Ighodaro*, Okenwa I. Okoli

High Performance Materials Institute, Florida State University, 2005 Levi Avenue, Tallahassee, FL 32310, United States

Received 16 October 2012; received in revised form 13 May 2013; accepted 31 May 2013

Available online 6 June 2013

Abstract

Regular channels of various sizes aligned in 2-D were fabricated in alumina using soft solder. The spaces between these channels were varied and their effects on the properties of alumina were investigated. It was found that these channels could significantly affect the fracture strength and elastic modulus of the specimen, depending on the channel diameter and spacing. After 3-point bend tests, it was seen that the presence of channels resulted in enhancement of modulus of rupture (MOR) and decrease in the scatter when compared to the solid specimen (specimen without channels). It was also observed that there exists an optimal spacing between the channels that imparts the highest MOR to the specimen. Beyond this value of spacing the MOR decreased, while the elastic modulus increased. The compressive strength also exhibited much less scatter for the porous specimen than for the solid specimen.

Published by Elsevier Ltd

Keywords: C. Fracture; C. Strength; D. Al_2O_3 ; E. Structural applications; Aligned channels

1. Introduction

Some of the desirable properties of advanced ceramics are their high values of stiffness, hardness corrosion resistance and specific strength, among various other desirable properties. However, the brittle nature of ceramics as well as the influence of cracks on them makes them less desirable for structural applications. According to Meyers and Chawler [1], fracture strength of a ceramic materials is highly influenced by the size, orientation, sharpness and distribution of defects such as cracks, pores, and inclusions present in them. Similar view has also been observed by Shabana et al. [2], where it was reported that cracks can be generated due to differential shrinkage during sintering, and can compromise the integrity of sintered materials. Another possible cause of cracking in sintered materials according to Chen et al. [3] is thermal gradient. Thermal gradient could give rise to density differential as well as differential shrinkage, and either may lead to crack generation. Since the distribution of cracks in a normal ceramic material is random, fracture strengths

of these materials are distributed over a wide range, thereby also reducing their reliability, in addition to strength reduction. Consequently, their desirability for structural applications is further reduced. To overcome these drawbacks the size of flaws must be significantly reduced as stated by Chen and Tuan [4].

Various methods for reducing the detrimental effects of cracks (and brittleness) in ceramics are emerging. Most of these methods are based on employing reinforcement such as laminated structures, functional gradients materials (FGMs), particle reinforcement, and fiber reinforcement on the ceramic matrix. A review surveying significant research efforts aimed to improve the fracture toughness of ceramics has been done by Ighodaro and Okoli [5]. She et al. [6] employed laminate designs involving Al_2O_3 and SiC phases to achieve crack deflection at the weak interfaces, thereby enhancing the bending strength, fracture energy and other mechanical properties of the laminate. In a similar work on laminates, Morgan and Marshall [7] observed crack arrest at the interface of alumina and Monazite layered composite. However, laminates may suffer from thermal cycling due to the differential thermal expansion between the phases [8] which may lead to crack generation. Lieberthal and Kaplan [9] employed spinel and nickel particles

*Corresponding author. Tel.: +1 850 408 2328; fax: +1 850 410 6342.

E-mail address: ighodos@eng.fsu.edu (O.L. Ighodaro).

(separately) for reinforcing alumina and reported significant enhancement of fracture strength brought about by grain boundary strengthening, crack bridging and crack deflection. Fiber reinforcements have also been employed to douse the effects of crack and enhance fracture properties of ceramics. Llorca and Singh [10] made ceramic composites reinforced with continuous fibers. They reported significant improvement in fracture toughness and crack growth resistance. However, due to the high sintering temperature of ceramics the fibers were degraded and their effectiveness in the composite was much reduced. Such mechanical property degradation has been reported by Pysher et al. [11]. They investigated the strength of ceramic fibers at elevated temperatures and reported that high temperature strength of SiC based fibers are limited by internal void formation and oxidation, while oxide fibers are degraded by intergranular glassy phase. Similar observations were also made by Llorca et al. [12] who reported that the ceramic fibers reinforced composites exhibited important reduction on toughness in air above 1000 °C.

The principle involved in all these methods is primarily the ability to provide or generate mechanism(s) capable of resisting fast propagation of cracks so as to enhance the mechanical properties of the ceramic material. However, another approach has been reported [13], in which 2-D channels were created in alumina, and it was shown that some of the 2-D porous preforms exhibited enhanced fracture strengths than the solid specimens. This effect was explained to be due to the ability of the channels to blunt out crack tips and also enhance more uniform heat distribution within the matrix during sintering and cooling from sintering temperature, thereby reducing crack population. Therefore, it seems important to find out the range of influence of each channel so as to enable the determination of an optimal channel configuration. The aim of this work therefore is to determine how the spacing and size of 2-D regular channels affect the fracture strength and stiffness of ceramics, using alumina as a typical popular ceramic material. It is expected that the results will be valuable in selecting channel sizes and spacing in porous preforms without sacrificing the mechanical properties. This will be helpful in designing porous preforms such as scaffolds, and also in assigning controlled volume fraction without degrading the ceramic preform, when fabricating metal reinforced ceramic composites.

2. Experimental procedure

Methods for fabricating continuous channels using carbon fibers and soft metals as sacrificial materials have been reported [13]. A brief review of the soft metal route, the method employed in this work, is presented here. Soft solder (McMaster, N.Y.) was woven into the required shape and sandwiched between ceramic powder. The mass was compacted uniaxially and transferred into a thermal chamber where the solder was heated to the molten state. Upon melting, the chamber was subjected to rotation (using a device fabricated for this purpose) at about 45 rpm to generate centrifugal forces in the chamber. This caused the molten sacrificial metal to flow

out leaving empty channels in the green compacted powder. The green compact now containing the profile of the desired channels was sintered at 1550 °C in air at a dwell time of 1 h to complete the porous preform fabrication.

Channels with various diameters: 250 µm, 315 µm, and 373 µm were fabricated in alumina matrix. The spacing of the channels were 2.5 mm, 3.3 mm and 4.1 mm. The complete set of specimens and their designations are shown in Table 1. Solid specimen ('S', which had no channels in it) was also made for comparison of properties. After the specimens cool to room temperature their densities were determined by Archimedes Principles, using water as the immersion fluid. They were then cut and polished to dimensions required for 3-point bend tests and uniaxial compression tests. The 3-point bend tests specimens had dimensions of 1.5 mm × 2.0 mm × 30.0 mm ($t \times b \times l$). Each specimen contained a central channel along the span and several others parallel to the breadth. Fig. 1 shows specimens containing the 373 µm channels. The specimens (C2, C3 and C4) are stacked to show the relative spacing of the channels in them. Modulus of rupture (MOR) (or fracture strength) of each specimen was determined by 3-point bend test using specimen span of 20.0 mm. The elastic strain of each specimen was determined using optical strain gage incorporated in the mechanical testing machine (Shimadzu AGS-J Mechanical Testing System). The (internal) walls of the channels as well as fracture surfaces were examined after the fracture tests using scanning electron microscope (SEM). The uniaxial compression tests were performed using specimens having dimensions 1.5 mm × 2.0 mm × 10 mm ($t \times b \times h$). Each specimen also has a central channel parallel to the height and other channels parallel to the breadth. Fig. 2 shows the set-up for the compression test. The gage length for compressive strain measurement was 7 mm. However, during the compression test, strain was not detected in many specimens before fracture, due to the small size of the compression specimens, and high stiffness of alumina. Therefore, results for compressive modulus are not included in this report.

3. Results and discussions

The measured densities of the specimens were approximately 98.3% ($\pm 0.58\%$) of their theoretical density of 3.96 g/cm³, without any significant differences due to channel diameter or spacing between the channels. The results of the fracture strengths (from 3-point bend tests) of the specimens are shown in Fig. 3. From Fig. 3(a) which shows the fracture strengths grouped in order of the channel sizes, it is seen that the solid specimen (S) which contains no channel exhibited lower mean fracture strength than all other specimens containing channels. Also the spread (or scatter) of fracture strength for the solid specimen is much wider than for all other specimens. It therefore seems that the channels also help enhance fracture strength reliability of these ceramic specimens.

Looking at specimens of Groups A, B and C in Fig. 3, a pattern seems to occur. The specimens with the least spacing of 2.5 mm (i.e. highest η ($=d/\delta$), see Table 1) – A2, B2 and C2 – exhibited the least mean fracture strengths in their

Table 1

Experimental specimens, their designations and features.

Specimen	Channel diameter (d) μm	Channel spacing (δ) mm	Channel ratio ($\lambda = d/t$)	Spacing ratio ($\eta = d/\delta$)	Channel fraction (f) %
A2	250	2.5	0.1667	0.1000	2.95
A3	250	3.3	0.1667	0.0760	2.64
A4	250	4.1	0.1667	0.0610	2.44
B2	315	2.5	0.2100	0.1260	4.68
B3	315	3.3	0.2100	0.0955	4.18
B4	315	4.1	0.2100	0.0768	3.86
C2	373	2.5	0.2487	0.1492	6.56
C3	373	3.3	0.2487	0.1130	5.85
C4	373	4.1	0.2487	0.0910	5.42
Solid (S)	–	–	–	–	–



Fig. 1. Specimen C series containing 373 μm diameter channels. The specimens C1, C2 and C3 are stacked to show the relative spacing of the channels: (a) side view showing several channels normal to the span; and (b) end view showing single channel along each specimen span.



Fig. 2. Set-up for compression test showing compression specimen between platens.

groups. Then the specimens A3, B3 and B4 having channels spaced at 3.3 mm had the highest mean fracture strengths in their groups. When the spacing of the channels increased to 4.1 mm (i.e. least $\eta (=d/\delta)$, see Table 1) – specimens A4, B4

and C4 – the mean fracture strengths decreased, although still higher than the strengths of the specimens A2, B2 and C2. This implies that there exists optimal channel spacing between 2.5 mm and 4.1 mm that imparts the highest fracture strength to the specimen. Fig. 3(b) shows the same results (as Fig. 3(a)) but here the specimens are arranged in groups of their channel spacing (the solid specimen is not shown here) to reveal more features exhibited by these specimens. It shows that at a given channel spacing of 2.5 mm, (Group 2), fracture strength reduces as channel diameter i.e. channel ratio ($\lambda = (d/t)$, see Table 1) increases. But when the channel spacing increased to 3.3 mm, (Group 3), with the same channel diameters, fracture strengths were significantly higher. Although there is no significant difference between the strengths of specimens in Groups 3 and 4 (channel spacing 3.3 mm and 4.1 mm respectively), the mean fracture strengths of specimens of Group 4 are generally lower than those of Group 3. This implies that the optimal spacing has already been exceeded (at 4.1 mm separation).

It has been reported [13] that the presence of the channels enhances uniformity of densification by helping more uniform heat distribution during sintering and while cooling down from sintering temperature, and this helps to reduce crack size population. Moreover, the presence of the channels limits the size of the largest crack as well as the crack sharpness, thus enhancing the fracture strength of the ceramic material. Therefore the channels are helpful in blunting the crack tips, limiting the crack lengths and narrowing the crack distribution. This is in agreement with the results of Deng et al. [14] where porous ceramics were used to enhance toughness by crack-tip blunting.

Also Kim and Kim [15] employed micro-void for enhancing toughness on epoxy resin. Flin et al. [16] reported toughening by artificial micro-voids. In their work they showed that artificial spherical defects in the range of 25 and 120 μm do not have any effect on fracture strength. In a similar work, Taylor et al. [17] studied the effect of stress concentration on the fracture strength of polymethylmethacrylate (PMMA) and reported that blunt notches with stress concentration factors less than 2 do not degrade fracture strength. Coble and Kingery [18] also reported that full potentiality of porous matrix can be realized only with matrix theoretical density or elongated and preferentially oriented pore structures. Therefore it may be reasoned that with the aligned channels presented in this work, crack blunting, enhanced toughness and higher strength can be expected, because the reduction of stress concentration enables the material to exhibit higher fracture strength. However, the size of the channels (or channel ratio, λ) may become large such that after blunting the crack tip the stress concentration induced by the channel (since stress concentration is also a function of channel size) may become large to cause strength degradation. This is the reason the Group 2 specimens shown in Fig. 3(a) exhibited reduction in fracture strength as channel diameter increased.

As the spacing of the channels increased their effectiveness in aiding uniform heat distribution is reduced. Also, since the longest crack will occupy the space between two adjacent channels, the largest crack size increases as the channel spacing increases. Thus, increasing the channel spacing beyond an optimal value tends to increase the crack size and crack population. Consequently, fracture strength begins a downward trend as exhibited by specimens shown in Fig. 3(a and b). It will also be noticed from Fig. 3(b) that the specimens of Group 3 (3.3 mm spacing) exhibited the least scatter in their fracture strength. When the spacing increased to 4.1 mm (Group 4 specimens) scatter in fracture strength increased. Since scatter is associated with random nature of flaws in the matrix; this also further supports the fact that the channels suppressed the detrimental effects of cracks. Thus the optimal channel spacing results in the highest fracture strength enhancement and least scatter. This is advantageous and desirable for structural materials.

The channels not only affected the fracture strength but also the elastic modulus of the specimens. Fig. 4 shows the elastic moduli of the various specimens. Fig. 4(a) (which shows the

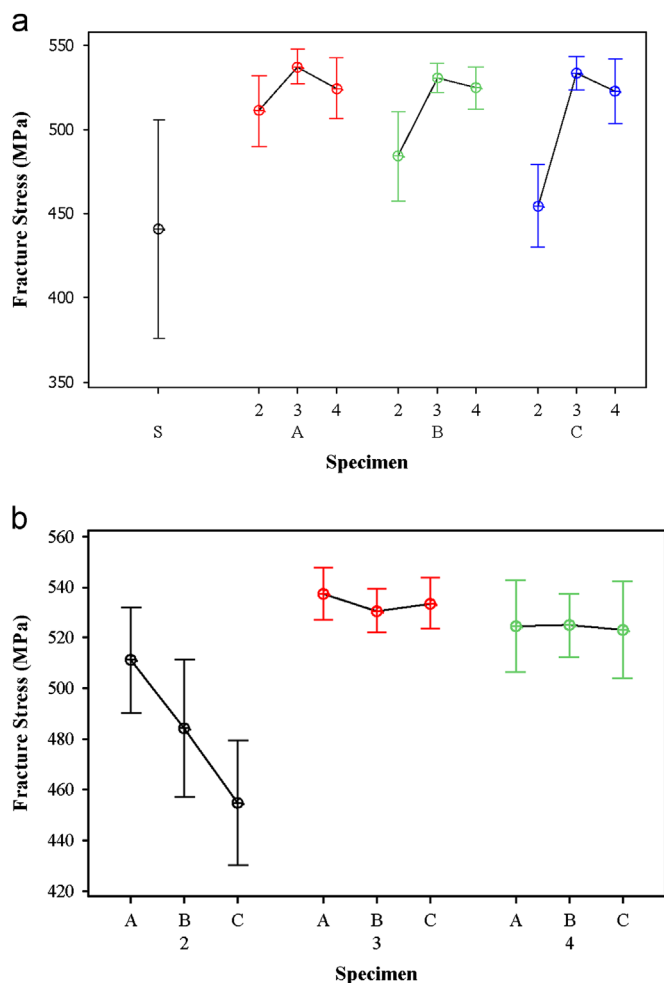


Fig. 3. Fracture strengths of specimens from 3-point bend test: (a) specimens arranged in groups of channel sizes; and (b) specimens arranged in groups of channel spacing (solid specimen, (S) not shown).

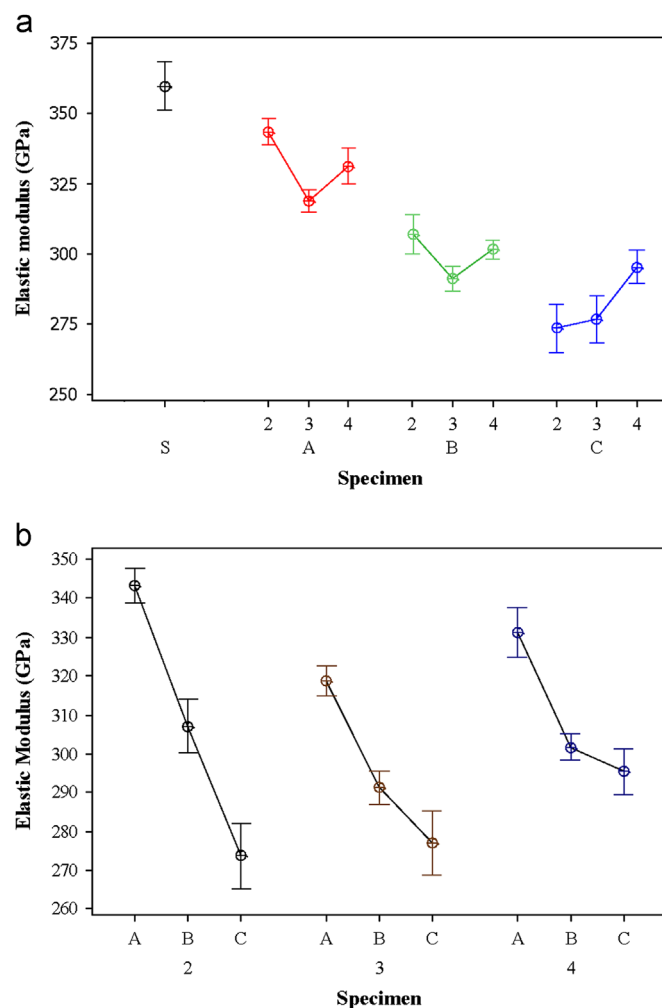


Fig. 4. Elastic modulus of specimens: (a) specimens in groups of channel sizes; and (b) specimens in groups of channel spacing (solid specimen, (S) not shown).

specimens in their groups of uniform channel diameter, i.e. Groups A, B and C) shows that the elastic modulus of the solid specimen (S) is higher than the modulus of all other specimens having channels. The specimens containing channels (as shown in Fig. 4(a)) reveal that the elastic modulus of the specimen decreased as channel size increased. This is expected since the increase in volume fraction of the channels increased the presence of void in the material, thereby reducing the volume (and consequently the moment of inertia) of the material. It is also noticed that there exists a turning point in each group at which the specimen exhibits minimum elastic modulus, and this corresponds to the specimen exhibiting the maximum fracture strength. Increasing the channel spacing beyond this turning point, elastic modulus began to increase. These happen because for any given channel size, the channel fraction decreased as the channel spacing increased, thus the volume of the material as well as its moment of inertia increased, leading to increase in modulus. From Fig. 4(b) it will be clearly observed that for a given channel spacing, elastic modulus is also significantly reduced as channel size increased. This occurs as a result of decrease in volume (and moment of inertia) as channel size increased (see Table 1). As the spacing of the channels continues to increase after the optimal spacing was exceeded, the fracture strength decreased while the elastic modulus increased.

Comparing the scatter associated with the fracture strengths and elastic moduli as shown in Figs. 3 and 4 respectively, it is obvious that the effect of the channels on the scatter on fracture strength is more pronounced than on elastic modulus, and this is due to the fact that cracks very significantly affect fracture strength more than they affect elastic modulus. Thus as the presence of the channels affected the emergence of cracks and also limited their possible sizes, the scatter in fracture strength of the specimen reduced, but scatter in elastic modulus was not significantly affected.

In Fig. 5(a and b), the results of the uniaxial compressive strengths are presented. Fig. 5(a) shows that the solid specimen (S) has significantly higher compressive strength, and more scatter than the porous materials. The less scatter observed in the porous materials could be attributed to the reduction in the effects of the cracks as discussed earlier. Generally compressive strength decreased as channel size increased. However, Specimen 3B (315 μm diameter, 3.5 mm spacing), possessed the highest mean compressive strength among the porous specimens. This is more clearly shown in Fig. 5(b) (which does not include the solid specimen 'S'). This is significant because this specimen configuration also had the highest fracture strength among its group in the 3-point bend test (see Fig. 3(a)). This tends to further support the existence of optimal channel configuration for each specimen.

The interaction between the channels and the matrix that gives rise to the observed mechanical features/properties was investigated microscopically by using scanning electron microscope (SEM). Fig. 6 shows an SEM image of a fracture surface containing a channel along the span of the 3-point bend specimen. The arrows show peripheral cracks along the circumference of the channel. This indicates that the channels

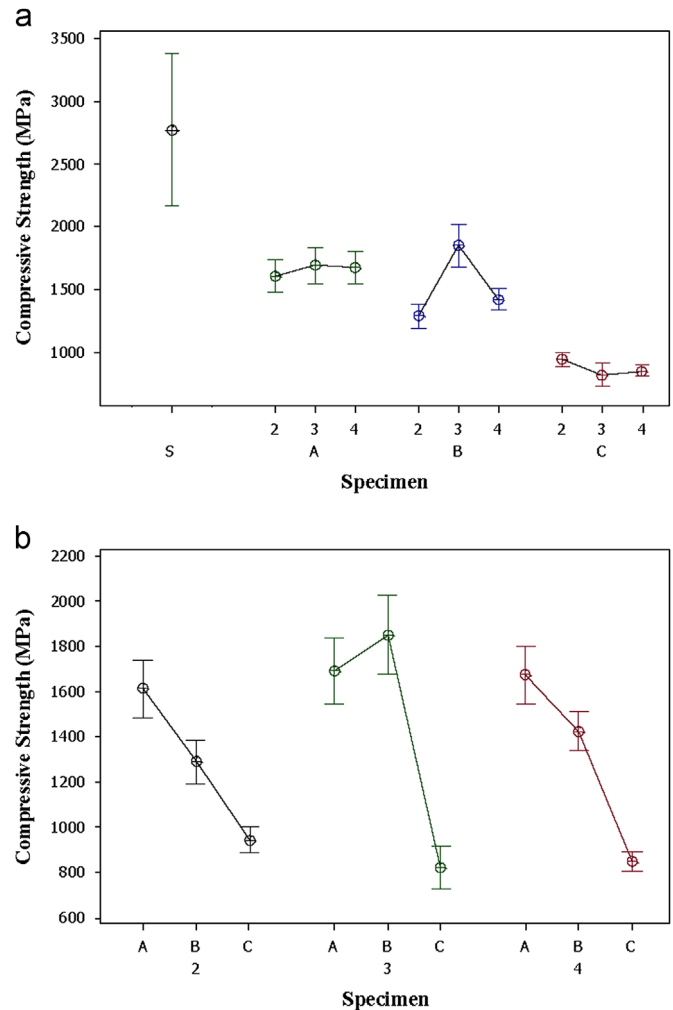


Fig. 5. Compressive strengths of specimens: (a) specimens arranged in groups of channel sizes; and (b) specimens arranged in groups of channel spacing (solid specimen, (S) not shown).

could actually arrest fast crack propagation and create multiple cracks since some of the cracks will terminate at the surface of a channel without causing failure. When a crack terminates without causing failure, another crack has to be initiated until failure occurs. The energy required to reinitiate a failure causing crack results in fracture strength enhancement as exhibited by the specimens tested in 3-point bending. Also, the potential of the channels to provide a crack path for the fracture event is beneficial since energy is consumed in this process, thereby preventing fast crack propagation across the specimen. To further highlight the role of the channels in the fracture process, Fig. 7(a) is displayed showing the interior wall of a channel after fracture. The arrows highlight crack path along the periphery of the channel. Severe fracture and grain pull-out can be seen at different locations along the wall. These are consequences of cracks terminating at the wall surface, and the multiple locations are evidence of multiple cracks. For comparison, the interior wall of a channel at a region far from the fracture surface is also shown in Fig. 7(b). Comparing Fig. 7(a) and (b), the significant damage on the

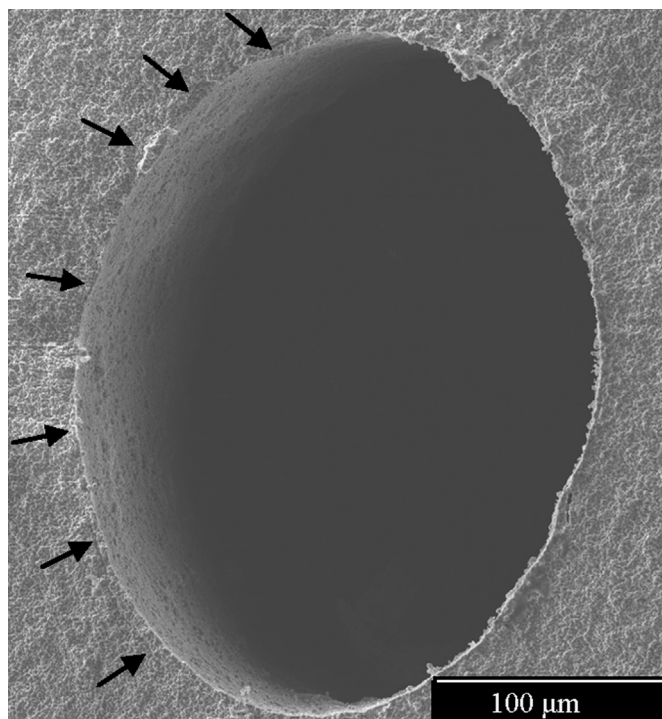


Fig. 6. Fracture surface of a specimen containing a central channel along the span. The arrows show peripheral cracks tracing the circumference of the channel.

wall of the channel around the fracture region shown in Fig. 7 (a) is evident of the energy consumption during fracture of the specimen containing the channel. This is a manifestation of fracture strength enhancement mechanism.

Even though these mechanisms may be present during compressive loading, the compressive strength of the solid specimen was higher than those of the porous specimens. This occurs because cracks tend to close up during compression. Therefore, their effects on compressive strength are not very significant. As such the aligned channels could not enhance the compressive strength of the porous alumina above their solid counterparts. However, the mechanisms (crack arrest and crack blunting), generated during compressive loading is responsible for the reduction in scatter exhibited in the compressive strength of the porous specimens.

4. Conclusions

This paper presents the investigation of the effects of regular 2-D aligned channels on some mechanical properties of alumina. The 2-D aligned networks of regular channels are found to possess the potential to significantly enhance the modulus of rupture (or fracture strength), elastic modulus and reliability of alumina. The enhancement in fracture strength was due to the interaction of the aligned channels within the matrix. The channels reduced the crack population and distribution, and consequently the detrimental effects of cracks were significantly reduced.

It was shown that the channels could provide preferential path for the cracks around the circumference of the channels at

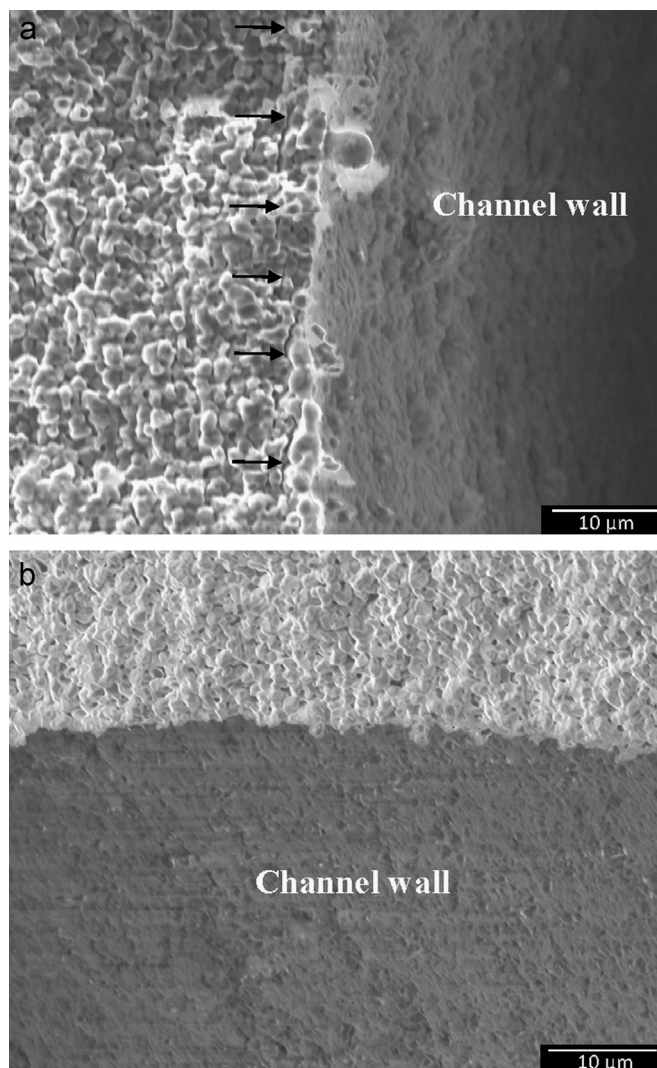


Fig. 7. SEM of fracture surfaces of specimens showing walls of the channels: (a) channel wall of a fracture specimen showing significant damage and peripheral crack path, and (b) channel wall of neatly cut specimen shows significantly less damage.

the fracture region. This causes more damage to be done around the channels during a fracture event thus reducing the rate of crack growth across the specimen. The energy consumed during this process is higher since the generation of multiple surfaces implies greater surface energies associated with the fracture. This high energy consumption translates to enhancement of fracture strength.

The spacing of the channels also significantly affects the properties, and an optimal spacing that brings about maximum enhancement of fracture strength exists for each channel size. However, the fracture strength and elastic modulus appear to move in opposite directions as the spacing of the channels is varied. Thus the specimen with the channel spacing that exhibited the highest fracture strength in each group (i.e. specimens with channel spacing 3.3 mm) exhibited the lowest elastic modulus. These results show that while both cracks and volume fraction affect the properties of alumina, fracture strength is more sensitive to cracks while elastic modulus is

more sensitive to volume fraction, and for this reason, the solid specimen, which normally contains the largest (sharp) crack/crack population exhibited the lowest fracture strength and highest elastic modulus.

The channels also helped in enhancing reliability (i.e. reducing scatter) in compressive strength values. However, the porous specimens exhibited significantly less compressive strength than the solid material because cracks tend to close up during compressive loads, suppressing their detrimental effects. Also during compressive loading, the effect of channels is more detrimental than the effect of cracks due to the higher volume fraction of the channels. As such the solid material was able to exhibit higher compressive strength than the porous materials.

An understanding of the effects of these channels on properties of brittle materials will help in designing high specific strength materials for structural applications. These results will also be useful in designing metal infiltrated ceramic matrix composites as well as biomedical scaffolds exhibiting optimal properties. Efforts are also being made to determine the nominal features (size, orientation, sharpness, etc.) of cracks in a solid ceramic specimen in relation to the processing method. This will enable the development of a model for the determination of optimal channel size and spacing.

References

- [1] M.A. Meyers, K.K. Chawler, *Mechanical Behavior of Materials*, Prentice-Hall, Inc., New Jersey, 1999.
- [2] Y.M. Shabana, et al., Modeling the evolution of stress due to differential shrinkage in powder-processed functionally graded metal–ceramic composites during pressureless sintering, *International Journal of Solids and Structures* 43 (2006) 7852–7868.
- [3] P. Chen, et al., Investigations in the compaction and sintering of large ceramic parts, *Journal of Materials Processing Technology* 190 (2007) 243–250.
- [4] R.Z. Chen, W.H. Tuan, Pressureless Sintering of $\text{Al}_2\text{O}_3/\text{Ni}$ Nanocomposites, *Journal of the European Ceramic Society* 19 (1999) 463–468.
- [5] O.L. Ighodaro, O.I. Okoli, Fracture toughness enhancement for alumina systems: a review, *International Journal of Applied Ceramic Technology* 5 (2008) 313–323.
- [6] J. She, et al., Multilayer $\text{Al}_2\text{O}_3/\text{SiC}$ ceramics with improved mechanical behavior, *Journal of the European Ceramic Society* 20 (2000) 1771–1775.
- [7] P.E.D. Morgan, D.B. Marshall, Ceramic composites of monazite and alumina, *Journal of the American Ceramic Society* 78 (1995) 1553–1563.
- [8] D. Padmavardhani, et al., Synthesis and microstructural characterization of $\text{NiAl}-\text{Al}_2\text{O}_3$ functionally gradient composites, *Intermetallics* 6 (1998) 229–241.
- [9] M. Lieberthal, W.D. Kaplan, Processing and properties of Al_2O_3 nanocomposites reinforced with sub-micron Ni and NiAl_2O_4 , *Materials Science and Engineering: A* 302 (2001) 83–91.
- [10] J. Llorca, R.N. Singh, Influence of fiber and interfacial properties on fracture behavior of fiber-reinforced ceramic composites, *Journal of the American Ceramic Society* 74 (1991) 2882–2890.
- [11] D.J. Pysher, et al., Strengths of ceramic fibers at elevated temperatures, *Journal of the American Ceramic Society* 72 (1989) 284–288.
- [12] J. Llorca, et al., Toughness and microstructural degradation at high temperature in SiC fiber-reinforced ceramics, *Acta Materialia* 46 (1998) 2441–2453.
- [13] O.L. Ighodaro, et al., Ceramic preforms with 2D regular channels for fabrication of metal/ceramic-reinforced composites, *International Journal of Applied Ceramic Technology* 9 (2012) 421–430.
- [14] Z.Y. Deng, et al., Reinforcement by crack-tip blunting in porous ceramics, *Journal of the European Ceramic Society* 24 (2004) 2055–2059.
- [15] N.H. Kim, H.S. Kim, Micro-void toughening of thermosets and its mechanism, *Journal of Applied Polymer Science* 98 (2005) 1290–1295.
- [16] B.D. Flinn, et al., Evolution of defect size and strength of porous alumina during sintering, *Journal of the European Ceramic Society* 20 (2000) 2561–2568.
- [17] D. Taylor, et al., The effect of stress concentrations on the fracture strength of polymethylmethacrylate, *Materials Science and Engineering: A* 382 (2004) 288–294.
- [18] R.L. Coble, W.D. Kingery, Effect of porosity on physical properties of sintered alumina, *Journal of the American Ceramic Society* 39 (1956) 377–385.